Wireless Personal Communications **4:** 277–298, 1997.

Dual-Space Diversity over Land Mobile Satellite Channels Operating in the L and K Frequency Bands*

W. ZHUANG[1], J.-Y. CHOUINARD[2] and D. MAKRAKIS[3]
[1]*Department of Electrical and Computer Engineering, University of Waterloo, Waterloo, Ontario, Canada N2L 3G1, (Tel.: 5198851211/5354; Fax: 5197463077; E-mail: wzhuang@bbcr.uwaterloo.ca);* [2]*Department of Electrical Engineering, University of Ottawa, 161 Louis Pasteur, Ottawa, Ontario, Canada K1N 6N5, (E-mail: chouinar@trix.genie.uottawa.ca;* [3]*Department of Electrical Engineering, Lakehead University, 955 Oliver Road, Thunderbay, Ontario, Canada P7B 5E1 (E-mail: dmakraki@flash.lakeheadu.ca)*

Abstract. Land mobile satellite communication systems at Ka/K band (30/20 GHz) are attracting more and more attention to researchers because of its frequency band availability and the possibility of using small earth stations and satellite antennas for the systems. However, the Ka/K-band communications also give significant challenges in the system design due to severe channel impairments expected from the satellite links. In this paper, K-band channel characteristics are studied and compared with those at L band. The channel is modeled as Rayleigh multipath fading with the line-of-sight (LOS) component following a lognormal distribution. The first and second-order statistics of the fading channel are studied. Dual-space diversity reception is investigated to combat the flat channel fading. The bit error rate performance of coherent binary phase shift keying (BPSK) with ideal bit and carrier phase synchronization over the fading channel at K band is evaluated theoretically and verified by computer simulations in the case with and without diversity reception.

Key words: Land Mobile Satellite Communications, channel modeling, diversity reception.

1. Introduction

The system concepts and technologies of introducing land mobile satellite (LMS) services at L band (1.5/1.6 GHz) have been developed and demonstrated throughout the 1980s. Presently they are at the stage of being transferred to the industry. However, inevitable congestion at L band, due to the limited bandwidth availability, eventually would fail to provide the services needed. Research work has been targeted towards future LMS systems that should be able to provide the users with cost-effective services, and with enough capacity to support a large number of users and their varied demands. Ka/K-band (30/20 GHz) mobile satellite communication systems provide such a promising solution. The systems have advantages including that:

i) large bandwidth is available;
ii) user equipment and earth station antennas can be significantly smaller and potentially less expensive than the equipment used in L-band systems.

On the other hand, Ka/K-band communications give significant challenges due to severe channel impairments expected from the satellite links, including significant rain attenuation, shadowing, multipath fading and potentially large frequency uncertainties in personal satellite communication systems. In order to facilitate the design of LMS communications systems and to predict the system performance with various coding and modulation schemes, it is important to establish statistical channel models for LMS communications. An LMS channel model at L

* This paper was presented in part at The Third International Mobile Satellite Conference (IMSC '93), Pasadena, California, June 16-18, 1993.

band has been developed based on experimental data [1]-[4]. The channel is characterized by a lognormally distributed line-of-sight (LOS) component and a Rayleigh distributed multipath component. In this paper, an effort is made to simulate the radio propagation channel at K band for mobile applications. Due to the fact that LMS channel experimental data at K band are very limited, we are not able to make a comprehensive prediction of the relevant fading statistics. From the mechanism of the LMS modeling at L and other frequency bands, it is reasonable to assume that the L-band channel model is also suitable to characterize the LMS channel at K band with the model parameters being appropriately scaled. A technique is developed here for mapping the average path loss (due to vegetation shadowing) to the statistical parameters of the lognormal distribution characteristic of the shadowed LOS signal component, based on the modified exponential decay (MED) model [5]. The effects of channel dynamics due to the mobility of the earth stations are taken into account in characterizing the second-order statistics of the fading channel, such as level-crossing rate (LCR) and average fade duration (AFD). Since the L-band data is available only for the downlink between the satellite and the mobile terminals, we study only the 20 GHz (K band) and 1.5 GHz (L band) downlink propagation channels, and our analysis is concentrated on multipath fading and shadowing. A clear sky condition is assumed, therefore, no rain/atmospheric attenuation is considered.

The bit error rate (BER) performance of coherent BPSK with ideal bit and carrier phase synchronization over the fading channel is analyzed as an example to demonstrate the effects of the channel statistics on the performance degradation of digital transmission. It is assumed that channel equalization techniques can be used to combat transmission performance degradation due to the propagation delay spread of the frequency-selective multipath fading channel. As a result, diversity reception is investigated as an effective way to combat flat channel fading. Although dual-space diversity reception requires two separate antennas, these antennas can be small at Ka/K band and be positioned close to each other (the wavelength at 30/20 GHz is only 1.0–1.5 centimeters). For multipath processes, the two antennas need only to be separated by half a wavelength to obtain two relatively independent signals [6]. For the LOS shadowed component, the separation of the two receiving antennas should be much larger than half a wavelength in order to achieve two independently shadowed LOS components, depending on the second-order statistics of the shadowing process. Previous work on the diversity reception is limited on Rayleigh, Rician or Nakagami fading channels [6]–[8]. In this paper, we consider the situation where the LMS channel is impaired by Rayleigh distributed multipath fading and where the LOS signal component is subjected to lognormally distributed shadowing. Both equal-gain (EG) combining and optimal maximum-ratio (MR) combining are considered for the L-band and K-band systems.

The objective of this paper is to model and analyze the K-band LMS channel in comparison with L-band channel, and to evaluate the BER performance of coherent BPSK in this environment with and without diversity reception. This paper is organized as follows. The first-order statistic description of the LMS channel is discussed in Section 2. Section 3 presents the second-order characteristics of the channel. An upper bound of the bit error rate of coherent BPSK with and without diversity reception over the fading channel is evaluated in Section 4, which is further validated by computer simulations. Conclusions of this work are presented in Section 5.

2. First-Order Statistics of the LMS Channel

It is well known that an LMS channel can be modeled as the summation of a diffused signal component following the Rayleigh distribution and an LOS signal component whose local mean follows a lognormal statistical distribution. The assessment of the LMS model has been carried out extensively at UHF and L bands. It has been shown that the lognormal distribution for the local mean fits experimental data for microwave mobile communications from 100 MHz to 11.2 GHz [9] and for land mobile satellite communications at 870 MHz and 1.5 GHz [1]-[2]. Here, we assume that the channel model is also valid for an LMS channel at 20 GHz according to the mechanism of multipath fading and shadowing random processes. The LMS channel at K band corrupts the signaling waveform transmitted through it by introducing a multiplicative amplitude gain and carrier phase shift, which can be expressed as

$$R(t) = r(t)\exp[j\theta(t)] = z(t)\exp[j\phi_L(t)] + g(t)\exp[j\phi_M(t)] \tag{1}$$

where $\phi_L(t)$ and $\phi_M(t)$ are carrier phase disturbances, uniformly distributed over $[0, 2\pi]$, for the LOS and multipath signal components respectively; $z(t)$ is a lognormally distributed random process representing the amplitude of the LOS signal; $g(t)$ is the envelope of the multipath component and is Rayleigh distributed; $r(t)$ and $\theta(t)$ represent the overall effects of the channel fading on the received signal envelope and carrier phase respectively. The probability density function (PDF) of the lognormally distributed LOS component $z(t)$ is given by [11]

$$p(z) = \begin{cases} \frac{1}{\sqrt{2\pi d_0}z}\exp\left[-\frac{(\ln z-\mu)^2}{2d_0}\right], & z > 0 \\ 0, & z \le 0 \end{cases} \tag{2}$$

where μ and $\sqrt{d_0}$ are the mean value and standard deviation of the normally distributed random process $\ln[z(t)]$. The PDF of the received signal envelope $r(t)$ is [1]

$$p(r) = \begin{cases} \frac{r}{b_0\sqrt{2\pi d_0}}\int_0^\infty \frac{1}{z}\exp\left[-\frac{(\ln z-\mu)^2}{2d_0} - \frac{r^2+z^2}{2b_0}\right] \mathrm{I}_0\left(\frac{rz}{b_0}\right) dz, & r \ge 0 \\ 0, & r < 0 \end{cases} \tag{3}$$

where b_0 is the power of the multipath signal and $I_0()$ is the zeroth-order modified Bessel function.

The effect of multipath fading and shadowing on the LMS system performance depends on the system operation environments. In open and tree-shadowed areas, multipath fading results from both specular reflection and diffuse scattering from the terrain surrounding the mobile earth station. With the increase of the RF frequency, the magnitude of the reflection coefficient and the ground conductivity also increase; therefore, more scattering at K band may come from small obstacles or terrain irregularities than those at L band [12]. On the other hand, the mobile antenna radiation patterns at K band are expected to be narrow enough to eliminate the problem to a great extent. For example, in L-band systems, a circularly-polarized crossed drooping-dipole antenna or a circularly-polarized conical log spiral antenna may be used as a mobile terminal receiver antenna. Such antennas are designed to be omni-directional in azimuth with a radiation pattern from 20 degrees to 60 degrees on the elevation plane for interference/multipath rejection [13]. However, for K-band systems, a mobile terminal receiver antenna can be designed as a microstrip Yagi array of microstrip patch elements or elliptical reflector-type antenna (to be used in conjunction with a separate TWTA or a solid state power amplifier), with an azimuth beamwidth of about 30 degrees and a 20 to 60

degree elevation range [14]. K-band antenna pointing systems enable the antennas to track the satellite for all normal vehicle maneuvers, so that the antenna beamwidth on the azimuth plane can be much smaller than that of the L-band antennas. As a result, in first approximation, it may be considered that multipath fading does not impair system performance at K band more than that at L band regarding the channel first-order statistics. In the following discussion, the power of the multipath component at K band is assumed to be the same as that at L band, i.e.,

$$b_{0\ 1.5GHZ} = b_{0\ 20GHz}\ . \tag{4}$$

At L band, the shadowing phenomenon mainly comes from the objects such as tree trunks. However, for the 20 GHz K-band signal, the shadowing on the LOS component may even come from the leaves and small branches of the trees whose dimensions are comparable with the wavelength (1.5 centimeters). The leaves and branches are capable of severely attenuating, refracting and diffracting the K-band signal and become significant contributors to the shadowing appearing in the channel. Therefore, it is expected that the downlink signal at K band will suffer more attenuation than that at L band due to much more significant shadowing in vegetation areas. At the present time, only preliminary results are available in the open literature for mobile applications at K band (e.g., [15]) and existing frequency scaling methods are not of straightforward applicability. An attempt has been made to estimate such a scaling factor using the Modified Exponential Decay (MED) model [5], developed from static propagation measurements through deciduous trees in Colorado. In this model, the fact that the shadowing attenuation (i.e., the path loss due to vegetation areas) increases as the RF frequency increases has been taken into account. Barts and Stutzman [16] applied the MED model to simulate an LMS channel, where the MED model is combined with the vegetative path length expressions of vegetation areas to predict the vegetative path loss based on physical path parameters and the link frequency. Since the MED model is based on static propagation measurements, it is used here to scale only the average path loss of the shadowing attenuation. The path loss, using the MED model, is given by

$$L = \alpha d_v \ \text{[dB]} \tag{5}$$

where d_v is the vegetative path length in meters intercepted by the LOS signal and α is the specific attenuation coefficient of the vegetation in decibel per meter (dB/m). The MED specific attenuation coefficient (dB/m) can be computed by the following equation [5]

$$\begin{aligned} \alpha &\approx 0.45 f^{0.284} && \text{for } 0 \le d_v \le 14 \\ \alpha &\approx 1.33 f^{0.284} d_v^{-0.412} && \text{for } 14 \le d_v \le 400 \end{aligned} \tag{6}$$

where f is the frequency (GHz). In the following, we consider the case of average shadowing between the environments with a few trees (light shadowing) and many trees (heavy shadowing) [2]–[3]. Therefore, it is reasonable to assume $0 \le d_v \le 14$. The scaling factors are

$$\begin{aligned} \alpha_{20GHz} &\approx \left(\frac{20}{1.5}\right)^{0.284} \alpha_{1.5GHz}\ (dB/m) \\ \alpha_{20GHz} &\approx 2.1 \alpha_{1.5GHz}\ (dB/m)\,. \end{aligned} \tag{7}$$

Expressions (4)–(6) and L-band parameters are used to calculate the K-band channel parameters in the following channel modeling. The model is then used to analyze the LMS

Table 1. Channel model parameters.

RF(GHz)	b_0	μ	$\sqrt{d_0}$
1.5	0.126	-0.115	0.161
20	0.126	-0.2415	0.3381

performance at K band. The amplitude attenuation of the lognormally distributed LOS component at L band equals [11]

$$A_{1.5GHz} = e^{x_{1.5}} \tag{8}$$

where $x_{1.5}$ is normally distributed with mean $\mu_{1.5}$ and variance $d_{0\ 1.5GHz}$. At K band with a carrier frequency equal to 20 GHz, the attenuation of the received LOS signal power in dBW is 2.1 times of that at L band (see (7)), that is,

$$A_{20}^2(dBW) = 2.1A_{1.5}^2(dBW)\,. \tag{9}$$

In terms of amplitude attenuation on a linear scale, (9) can be rewritten as

$$\begin{aligned} 20\log_{10} A_{20} &= 2.1(20\log_{10} A_{1.5}) \\ \Rightarrow A_{20} &= A_{1.5}^{2.1} \\ \Rightarrow e^{x_{20}} &= e^{2.1x_{1.5}} \\ \Rightarrow x_{20} &= 2.1x_{1.5}\,. \end{aligned} \tag{10}$$

The mean and standard deviation at 20 GHz are then equal to

$$\begin{aligned} \mu_{20} &= 2.1\mu_{1.5}, \\ \sigma_{20} &= 2.1\sigma_{1.5}, \\ \sqrt{d_{0\ 20GHz}} &= 2.1\sqrt{d_{0\ 1.5GHz}}\,. \end{aligned} \tag{11}$$

For the case of average shadowing, the parameters of the L-band (1.5 GHz) mobile satellite channel are shown in Table 1 [1]–[4]. Their calculations are based on measurements carried out in Ottawa, Canada. The INMARSAT's MARECS A satellite was used in the experiments. The elevation angle from Ottawa to the satellite was approximately 20 degrees. From (4) and (11), the parameters of the first-order statistics of the LMS channel at K band are obtained and listed in Table 1. It should be pointed out that this is an estimate model to predict the path loss due to shadowing and multipath fading, and that further modifications may be necessary when more experimental data at K band become available.

Figure 1 is a software simulation model of the LMS channel. The low-pass (LP) filtered Gaussian noise processes are generated by summing a large number of sine waves [9]. The bandwidth of the LP filters is B_1 for the shadowing component and B_2 for the multipath component. In the following computer simulations, taking the vehicle speed of 43.2 kilometers/hour as an example, the maximum Doppler frequency shifts (which is the bandwidth of the complex Gaussian noise generator for multipath fading, i.e., B_2) are 60 Hz for the L-band signal and 800 Hz for the K-band signal. From measurement data at L band, it is found that the multipath fading process varies 20 times faster than the shadowing process [10]; therefore, the bandwidth of the Gaussian noise generator for the shadowing components (i.e., B_1) is taken as 1/20 of B_2, that is 3 Hz for L band and 40 Hz for K band. The signal sampling rate is

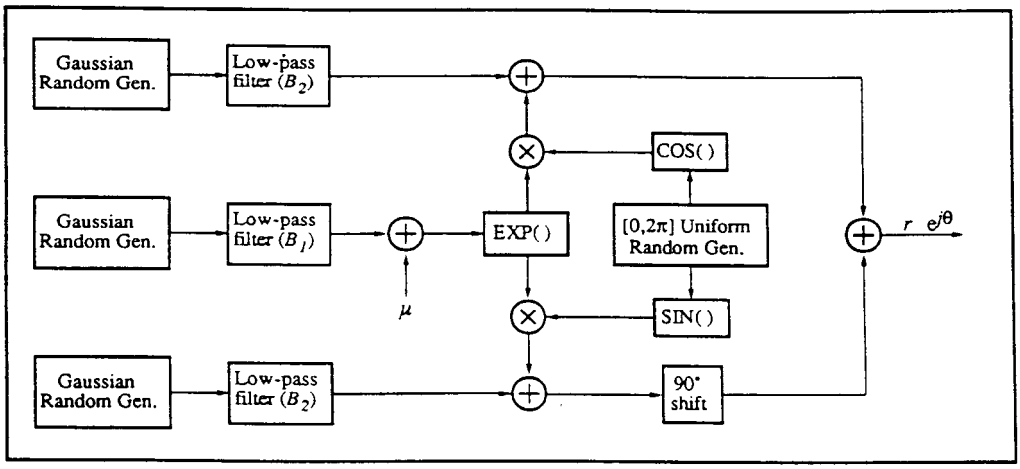

Figure 1. Functional block diagram of the shadowed LMS channel model.

Table 2. Ratio of LOS signal power to multipath signal power.

RF(GHz)	analytical (dB)	simulation (dB)
1.5	5.21	5.20
20	4.88	4.88

2400 Hz. Each simulation result is obtained based on over 250,000 sampled data. The signal amplitude level is relative to the LOS signal component without shadowing (0 dB) in the case of single channel reception, therefore, only the path loss due to shadowing and multipath fading is taken into account. In the simulation model, the amplitude fading $r(t)$ and carrier phase jitter $\theta(t)$ are generated at the same time, however, only the effect of the amplitude fading is considered in the transmission performance analysis.

The ratio of the LOS signal average power $\exp(2\mu + 2d_0)/2$, which can be derived from (2), to multipath signal power b_0 is a parameter similar to the K-factor in a Rician channel. Table 2 gives the analytical values and the simulation results of the ratios for the L-band and K-band signals using the parameters given in Table 1. The simulation results agree very well with the analytical values. The received K-band signal has an additional 0.23 dB loss of the ratio compared with the L-band signal. Figure 2 shows the cumulative distribution of the received L-band and K-band signal envelopes. The analytical results are obtained from equation (3). The results show that the K-band signal has more attenuation than the L-band signal, which agrees with the earlier discussion. In this specific propagation environment defined by the parameters of Table 1, although the K-band signal has an additional 1.0 dB path loss approximately, due to shadowing, compared to the L-band signal, in the area of deep fading (received signal amplitude level less than -12.5 dB), the K-band signal can experience more than 4.0 dB additional loss than the L-band signal. Note that it is the deep fading area that causes a dramatic BER performance degradation of an LMS communications system.

Figure 3 gives the cumulative distribution of the received LOS signal envelopes at L band and K band respectively. The analytical values are obtained according to (2). In general, the K-band signal is expected to experience more shadowing attenuation than the L-band signal

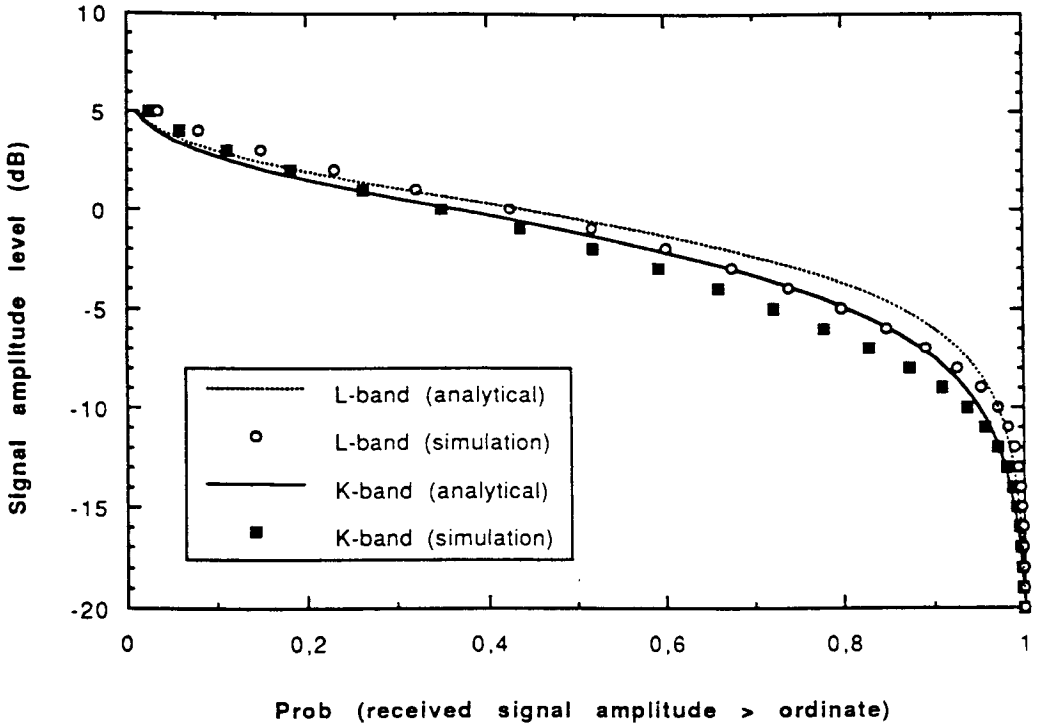

Figure 2. Probability distribution of the received signal envelope.

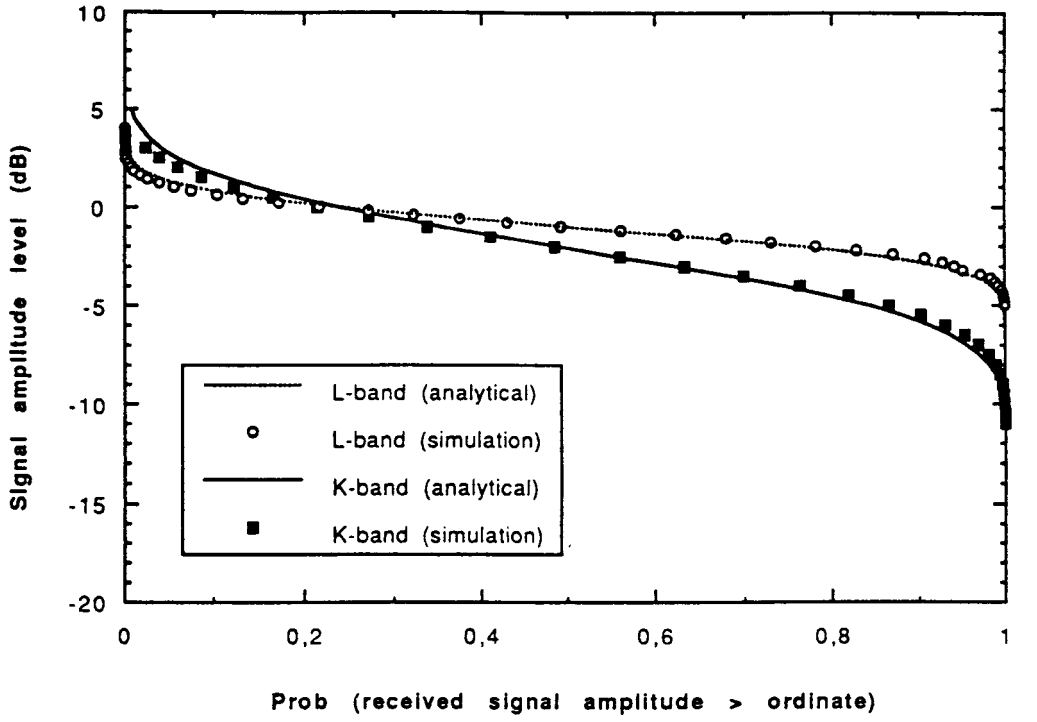

Figure 3. Probability distribution of the received LOS signal envelope.

Table 3. Amplitude level of shadowed LOS components.

RF(GHz)	P =70%	P = 80%	P = 90%
1.5	-1.66 dB	-2.07 dB	-2.55 dB
20.0	-3.65 dB	-4.53 dB	-5.85 dB

(especially in the deep fading region), which is clearly illustrated in the figure. The signal at K band has an additional loss of up to 6.0 dB in comparison with the L-band in the weak signal range (which is the most important range for fade margin calculation). It is noticed that in some cases the shadowed K-band LOS signal is stronger than the corresponding L-band signal. This phenomenon is verified by experimental data [17] and can be explained as follows. The K-band signal has much shorter wavelength than the L-band signal does. In the case of average shadowing, if the vegetative area happens to form some unshadowed "tunnels" (which are equivalent to waveguides) whose dimensions are much smaller than the L-band signal wavelength but larger than the K-band signal wavelength, then the K-band LOS signal can pass through whereas the L-band signal cannot. This would give to the K-band signal more powerful penetrating capability than the L-band signal, and therefore the signal can propagate through some vegetative areas and reach the receiver antenna.

In addition, the following fact should also be taken into account. There are dual effects of tree shadowing on the LOS signal component: attenuation and scattering. With the increase of the signal carrier frequency, its wavelength decreases, therefore, trees having the same vegetative path length intercepted by the LOS signal will attenuate the K-band signal more than the L-band signal. At the same time, the various LOS signal components scattered from the trees arrive at the receiver antenna through multiple paths. This is different from the Rayleigh multipath fading because the reflectors and scatterers (such as tree leaves and branches, power lines, etc.) exist only between the transmitter and the receiver. The scattering from the trees may increase the LOS signal amplitude. In the case of occasional propagation environment with only a few trees, the scattering phenomenon may have more effect on the LOS signal than the shadowing attenuation (we can expect a very small tree depth intercepted by the signals). Because the small tree branches (with the branch dimensions comparable to the signal wavelength) can reflect or diffuse the K-band signal, it is possible that occasionally the received K-band signal will be stronger than the L-band signal. As a result, the amplitude of the LOS signal at K band will be larger than at L band. From Figure 3, we also notice that there is a certain probability that the shadowed signal component will be even stronger than the unshadowed LOS component (0 dB). The results shown in Figure 3 are based on the mathematical modeling of the lognormally-distributed shadowing process which is derived from experimental data. The model parameters are obtained according to the best fit between the mathematical model and the measured data [1]. Therefore, the strong signal region (> 0 dB) may not represent the real shadowing process. From Figure 3, it can be observed that the average LOS component attenuation due to shadowing is 0.77 dB at L band and 1.10 dB at K band. Table 3 shows the amplitude level of the shadowed LOS components at the cumulative probabilities of 70%, 80% and 90%. The results shown in Figures 2 and 3 are based on an average shadowing propagation environment. The path loss difference between the L- and K-band signals depends on the channel propagation conditions.

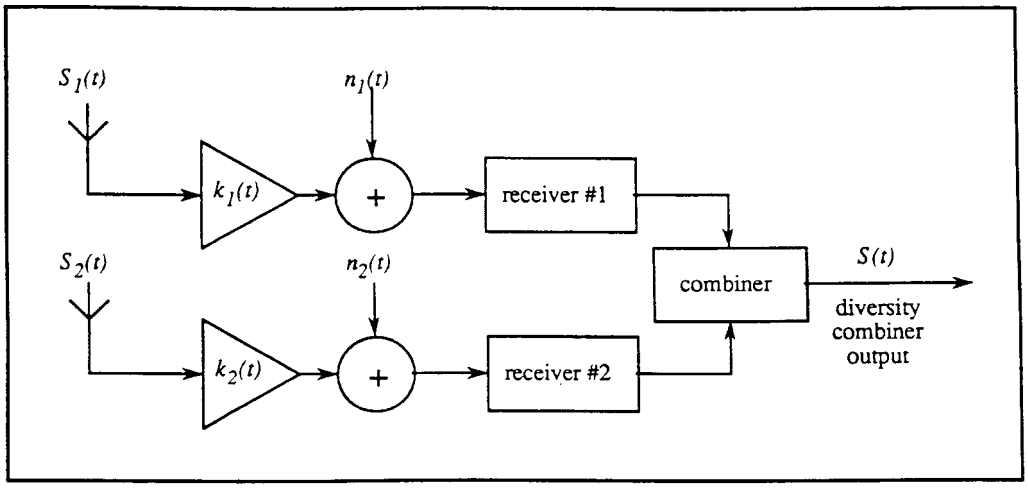

Figure 4. Simplified block diagram of dual=space diversity reception

Figure 4 depicts a simplified block diagram of a dual-space diversity reception system. The signal envelope $r(t)$ at the output of an equal gain diversity combining system is equal to

$$r(t) = r_1(t) + r_2(t)\,. \tag{12}$$

In (12), we have assumed that the diversity combining system can track the phase jittering appearing on the received signals and removes it. The PDFs of $r_1(t)$ and $r_2(t)$ are given in (3). The two antennas are assumed to be properly located so that the signals received through them (including both multipath component and LOS component) are uncorrelated. Since the shadowing process varies at a much slower rate than the multipath fading process, the separation between two antennas should be much larger than half a wavelength. For example, if the multipath fading is 20 times faster than the shadowing, approximately 10-wavelength separation between the antennas are required. In this case, the PDF of $r(t)$ is equal to [11]

$$p_2(r) = \int_0^r p_1(x)p_1(r-x)dx\,. \tag{13}$$

Combining (13) with (3), the PDF of the combined signal envelope $r(t)$ can be computed. Figure 5 shows the numerical analysis results as well as the computer simulation results of the cumulative probability distribution of the received envelope $r(t)$ at L and K bands. Comparing the distributions shown in Figure 5 and Figure 3, we observe that the diversity reception reduces the channel fading by approximately 5.0 to 9.3 dB at L and K bands. The improvement is much more significant as the received signal amplitude levels decrease (i.e., in the deeper fading area). The difference in the received signal envelope levels between L and K bands over non-deep fading region is not as significant as over the deep fading region due to: i) the low joint probability that both multipath components will fade simultaneously; and ii) the assumption that the power of the received multipath signal at K band is about the same as at L band.

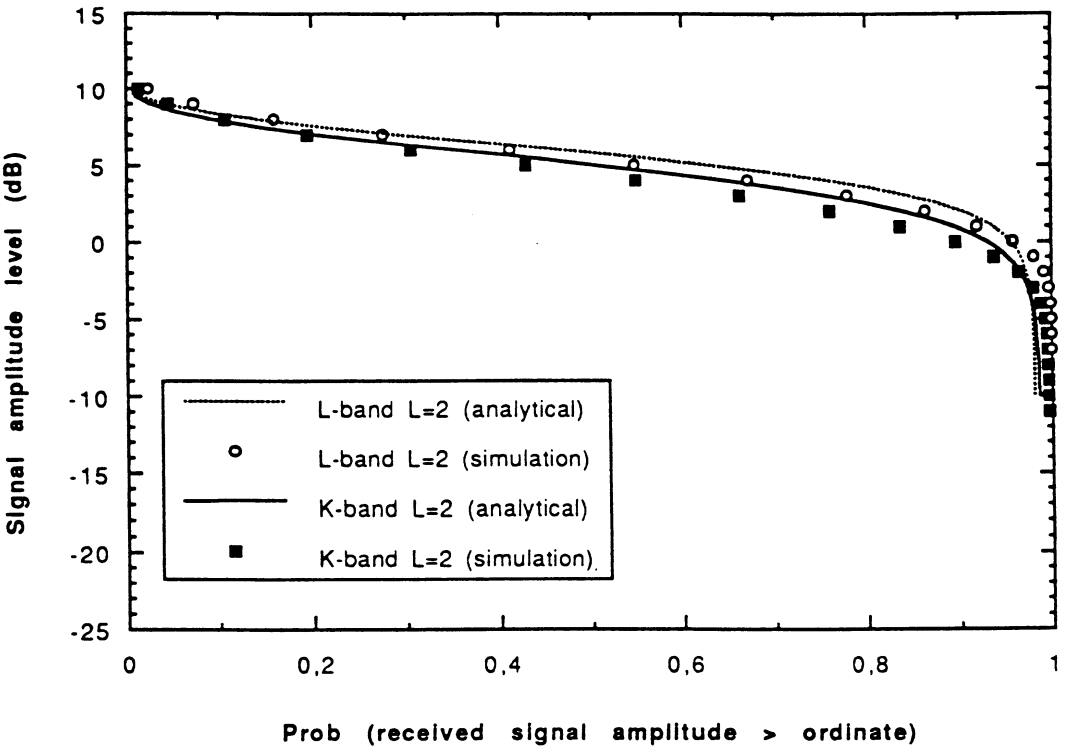

Figure 5. Probability distribution of the received signal envelope with dual-space equal gain diversity reception.

3. Second-Order Statistics of the LMS Channel

Second-order statistics are used to describe the time-dependent fading channel behaviour, which include level-crossing rate (LCR) and average fading duration (AFD). LCR is defined as the expected rate at which the envelope crosses a specified signal level Λ with a positive slope. It is given by the following equation

$$LCR(r = \Lambda) = \int_0^\infty \dot{r}\, p(\Lambda, \dot{r}) d\dot{r} \tag{14}$$

where $\dot{r}$ represents the time derivative of $r(t)$ and $p(\Lambda, \dot{r})$ represents the joint probability density function of $\dot{r}(t)$ and $r(t)$ at $r(t) = \Lambda$. It has been found that the LCR increases as the maximum Doppler frequency shift of the input signals increases. The maximum Doppler shift depends on the vehicle speed, the angle between the transmitter-receiver axis and the relative speed vector of the earth station, as well as the RF frequency of the system. The details of the mathematical formula for calculating LCR are discussed in [18].

The duration of a signal fade determines the number of bits that will be lost during the fade. The signal fade duration is affected by several factors, among which are the speed of the mobile vehicle and the RF operating frequency. The relationship between the average duration of the signal fade and the expected number of crossings per second, at a particular signal level Λ, can be stated as

$$LCR(r = \Lambda) = \frac{P(r \leq \Lambda)}{AFD(r = \Lambda)} \tag{15}$$

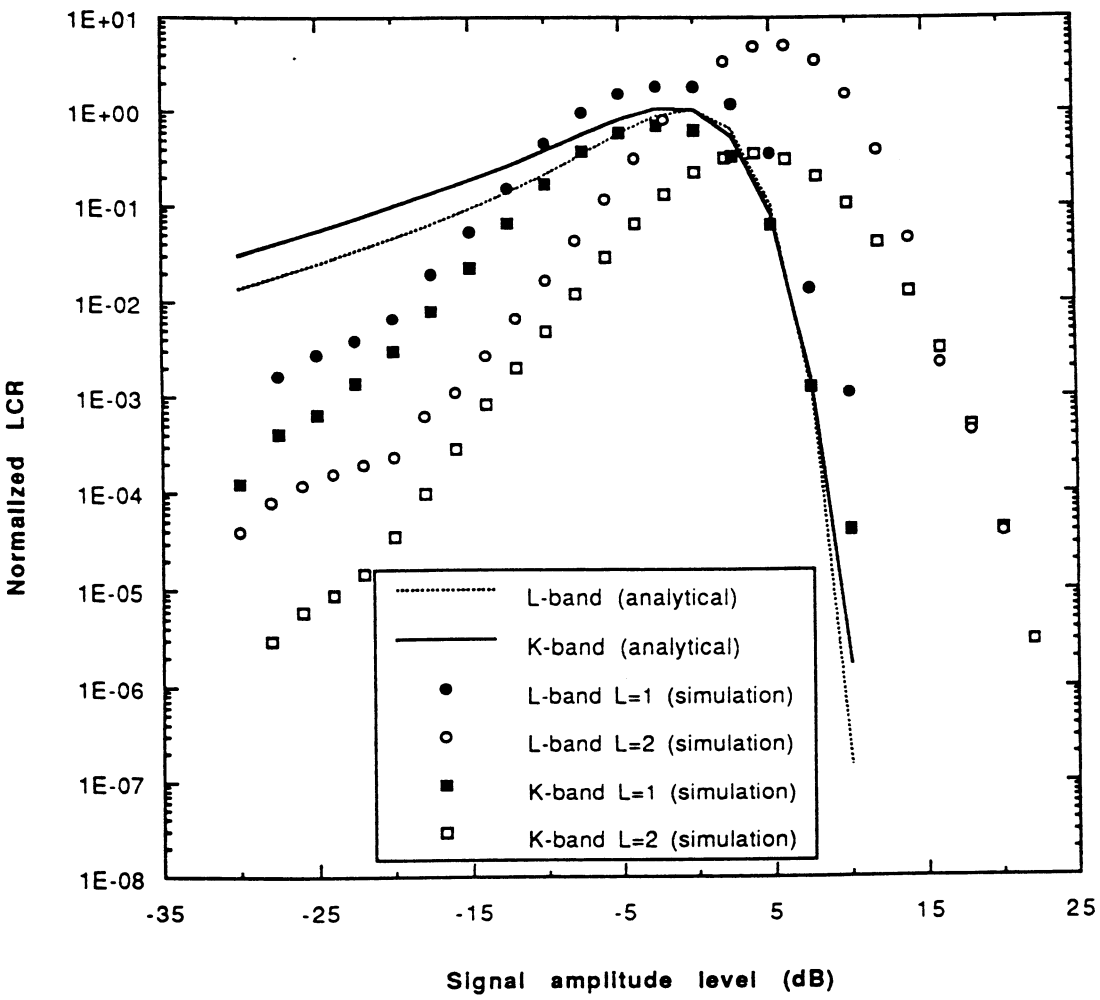

Figure 6. Normalized LCR with and without diversity reception.

where $P(r \leq \Lambda)$ represents the expected amount of time when the function $r(t)$ is below level Λ in 1 second, and $AFD(r = \Lambda)$ indicates the average duration of fades below level Λ in 1 second also.

In the case of multipath Rayleigh fading with lognormal shadowing, the LCR normalized with respect to the maximum Doppler frequency shift F_{dm} is [1]

$$\begin{aligned} LCR_n(r = \Lambda) &= LCR(r = \Lambda)/F_{dm} \\ &= \sqrt{2\pi(1-\rho^2)} \left[\frac{b_0 \left(b_0 + 2\rho\sqrt{b_0 d_0} + d_0\right)^{\frac{1}{2}}}{b_0(1-\rho^2) + 4\rho\sqrt{b_0 d_0}} \right] p(r) \end{aligned} \tag{16}$$

where ρ is the correlation coefficient between the envelope $r(t)$ and the envelope rate of change $\dot{r}(t)$. The corresponding normalized AFD is

$$AFD_n(r = \Lambda) = AFD(r = \Lambda)F_{dm} = \frac{1}{LCR_n} \int_0^{\Lambda} p(r)\, dr\,. \tag{17}$$

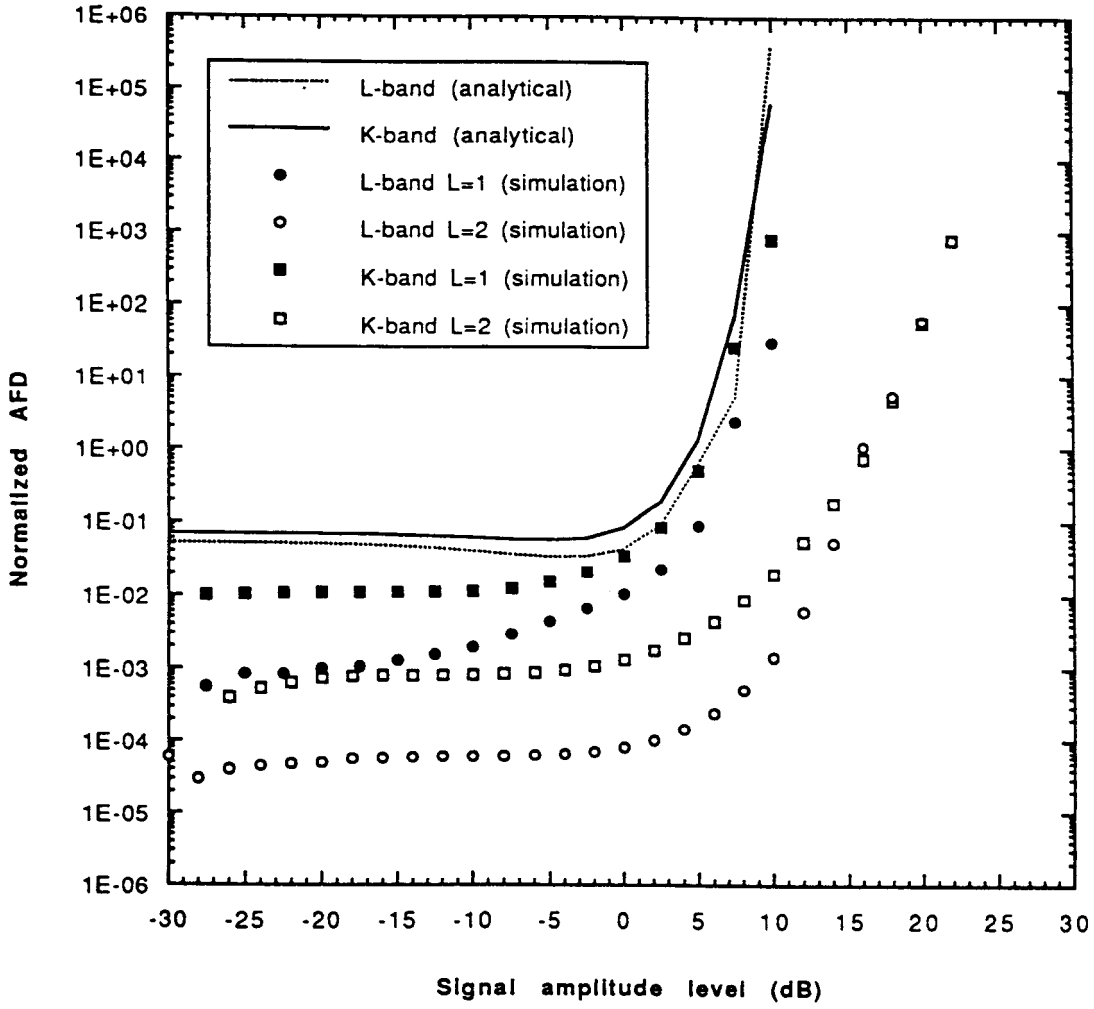

Figure 7. Normalized AFD with and without diversity reception.

The analytical values and simulation results of the second-order characteristics (LCR and AFD), with and without diversity, are shown in Figures 6 and 7. The results show that the maximum values of the normalized LCRs, for both the L band and K band cases, are very close to 1.0, which means that the LCRs increase almost linearly with the increase of the vehicle speed or the increase of the RF operating frequency. The analytic values are obtained with $\rho = 0$, i.e., it is assumed that there is no correlation between $r(t)$ and $\dot{r}(t)$. In reality, there exists some correlation between $r(t)$ and $\dot{r}(t)$, and ρ may not be a constant, which can be further confirmed by the experimental data (see Figures 2–7 of [1]). That explains the slight differences observed between the simulation results and the analytical curves of Figure 6.

From the simulation results, a number of observations can be made:

i) In the case of no diversity reception, the signal level at K band is attenuated more severely than that at L band, taken into account that the K-band signal has more shadowing attenuation;

ii) Diversity reception reduces the normalized AFD by more than 10 times, i.e., the deep fading duration is dramatically reduced, therefore, we can expect that the LMS system performance will be significantly improved, especially when coded modulation with Viterbi decoding is used;

iii) At a lower signal amplitude level (i.e., < 0), the normalized LCR is reduced by diversity at both L and K bands; at a higher signal amplitude level (i.e., > 0), the normalized LCR is increased by diversity. This shows that diversity reception reduces the likelihood of deep fading;

iv) The fading impairment is mitigated more at K band than at L band by the diversity reception.

In summary, the dynamic behaviour (i.e., fading rate, LCR and AFD) of the LMS channel due to shadowing and multipath fading at K band, caused by the mobility of the earth stations, are characterized in the K-band channel modeling by: i) using the same statistical model (but with modified channel parameters) as that of the L-band LMS channel developed on the basis of experimental data for mobile applications; and ii) increasing the Doppler frequency shift proportionally to the increase of the RF carrier frequency. The second-order statistics are crucial to the performance of the communications systems.

4. Performance Evaluation of Coherent BPSK

The theoretical analysis on the transmission performance of coherent BPSK presented in this Section is verified by Monte Carlo computer simulations. In the simulations, the number of information bits transmitted through the system for each average ratio of energy per received information bit to one-sided noise density, i.e. E_b/N_0, is chosen in such a way that the simulated BER performance results are within the 90 percent confidence interval $[0.5BER, 2.0BER]$. The BER confidence interval depends on the number of occurrences of error bits as well as the number of fading cycles that the LMS system experiences.

4.1. Single Channel Reception

It is assumed that the effects of carrier phase jitter due to the fading channel can be removed. Tracking of the phase fluctuations due to fading may be difficult at K-band since the fading rate is considerably faster as compared to the L-band, and might require the development of some new technology. However, since investigation of carrier phase synchronization techniques is beyond the scope of this work, we make in our study the assumption mentioned earlier. Here we are interested in the effects of signal envelope fading on the BER performance of coherent BPSK. In the following, only amplitude fading is taken into account. The bit error rate P_e of a coherent BPSK signal in an AWGN channel is given by [7]

$$P_e = \frac{1}{2}\,\mathrm{erfc}\left(\frac{r}{\sqrt{2\sigma_N^2}}\right) \tag{18}$$

where σ_N^2 is the variance of input Gaussian noise and $\mathrm{erfc}()$ is the complementary error function [11]. An upper bound for the instantaneous bit error rate, i.e. P_e^{in}, can be calculated by upper-bounding the complementary error function as follows [7]

$$P_e^{in} \leq \frac{1}{2}\exp\left(-\frac{r^2}{2\sigma_N^2}\right). \tag{19}$$

An upper bound, P_e^{av}, for the average bit error rate is obtained by combining (3) with (19),

$$P_e^{av} \leq \frac{1}{2}\frac{1}{\sqrt{2\pi d_0}}\int_0^\infty\int_0^\infty \frac{1}{z}\exp\left[-\frac{(\ln z-\mu)^2}{2d_0}\right] \exp\left(-\frac{z^2}{2b_0}\right)\frac{r}{b_0}\exp\left[-\frac{r^2}{2}\left(\frac{1}{b_0}+\frac{1}{\sigma_N^2}\right)\right]\mathrm{I}_0\left(\frac{rz}{b_0}\right)\,dr\,dz\,. \tag{20}$$

Furthermore, it can be shown that

$$P_e^{av} \leq \frac{1}{2}\frac{1}{\sqrt{2\pi d_0}}\frac{\sigma_N^2}{b_0+\sigma_N^2}\int_0^\infty \frac{1}{z}\exp\left[-\frac{(\ln z-\mu)^2}{2d_0}\right]\exp\left[-\frac{z^2}{2(b_0+\sigma_N^2)}\right]\,dz\,. \tag{21}$$

Similarly, if only the LOS component is considered, then

$$P_e^{av} \leq \frac{1}{2}\frac{1}{\sqrt{2\pi d_0}}\int_0^\infty \exp\left[-\frac{z^2}{2\sigma_N^2}-\frac{(\ln z-\mu)^2}{2d_0}\right]\,dz\,. \tag{22}$$

The analytical upper bounds as well as the simulation results for the bit error rate of a coherent BPSK system at L and K bands are presented in Figure 8. This figure shows the bit error rate due to amplitude fading of the LMS channel. At a BER of 10^{-3}, the communication system, when operating at K band, loses 3.5 dB as compared with the L band.

4.2. Diversity Reception

The performance of a coherent BPSK system with dual-space diversity reception operating in an LMS channel at L band and K band is studied in the following. The model of a dual-space diversity combiner is shown in Figure 4. The ith received signal $S_i(t)$ at the antenna ($i = 1, 2$) is

$$S_i(t) = r_i(t)\exp[j\theta_i(t)]\cos\{j[2\pi f_c t + \psi_m(t)]\} + n_i(t) \tag{23}$$

where f_c is the carrier frequency, $\psi_m(t) = 0$ or π is the information-carrying phase, $\theta_i(t)$ and $r_i(t)$ are the random carrier phase jitter and the faded signal envelope respectively from the ith antenna. In (23), $n_i(t)$ represents the additive white Gaussian noise (AWGN) with one sided power spectral density N_0. If we assume that the two diversity branches are locally coherent with the carrier phase jitter due to the channel fading, i.e., we assume that each of the diversity branches has a perfect carrier phase recovery, then the diversity branch gain $K_i(t) = k_i(t)\exp[-j\theta_i(t)]$, and the resultant predetection signal at the output of the diversity combiner is

$$S(t) = \sum_{i=1}^{2} k_i(t)[S_i(t) + n_i(t)]\exp[-j\theta_i(t)]\,. \tag{24}$$

The input signal at baseband is

$$S_b(t) = [k_1(t)r_1(t) + k_2(t)r_2(t)]\cos[\psi_m(t)] + N(t) \tag{25}$$

where $N(t)$ is the equivalent low-pass filtered Gaussian white noise.

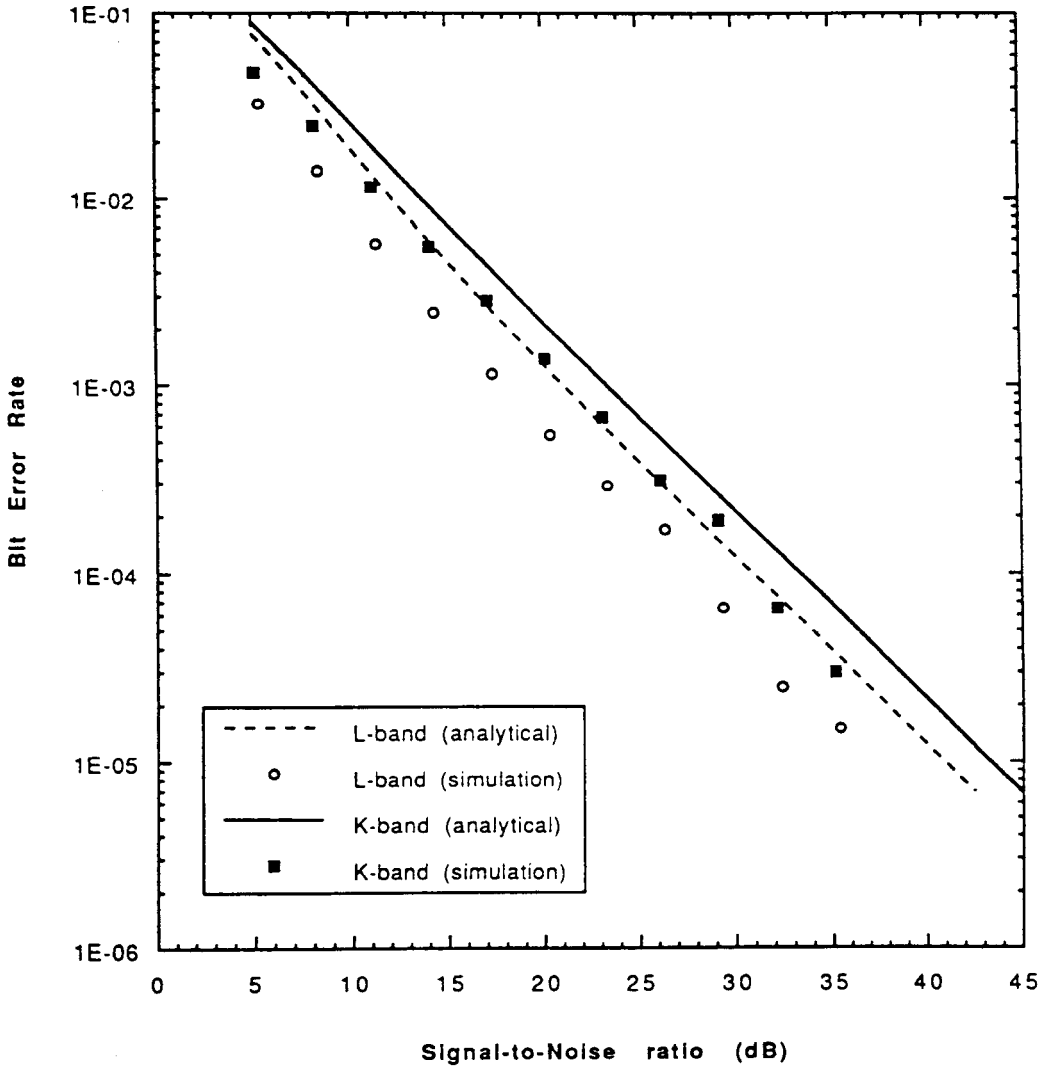

Figure 8. BER performance of coherent BPSK in LMS channel with single channel reception (average shadowing).

i) Equal Gain Combining

Equal gain combining is the simplest diversity combining technique. In this case, the gain $K_i(t)$ in Figure 4 is

$$K_i(t) = \exp[-j\theta_i(t)], \qquad \text{for } i = 1, 2 \tag{26}$$

which removes the jitter due to fading process from the signal phase. Therefore,

$$S_b(t) = [r_1(t) + r_2(t)] \cos[\psi_m(t)] + N(t)\,. \tag{27}$$

Since the phase jitter has been eliminated, only the amplitude fluctuations affect the performance. From (3), (13) and (19), the upper bound of the average bit error rate can be obtained from the following equation.

$$P_e^{av} \leq \frac{1}{2}\int_0^{\infty} \exp\left(-\frac{r^2}{2\sigma_N^2}\right) p_2(r)dr \tag{28}$$

and the average signal-to-noise ratio SNR^{av} of the received signal is equal to

$$SNR^{av} = \int_0^{\infty} \frac{r^2}{2\sigma_N^2}\, p_2(r)dr\,. \tag{29}$$

Figure 9 shows the bit error rate of a coherent BPSK system with equal gain combining. The analytical results are obtained by solving (28) and (29) numerically. Compared to the BER performance without diversity reception (Figure 8), at a BER of 10^{-3}, the receiver performance is improved approximately by 6.8 dB at L band, 8.4 dB at K band; and at a BER of 10^{-4}, approximately by 12.1 dB at L band, 14.0 dB at K band respectively.

ii) Maximum Ratio Combining

Maximum ratio diversity combining produces the best performance. With maximum ratio diversity, the branch gain $K_i(t)$ of Figure 4 is equal to [19]

$$K_i(t) = r_i(t)\exp[-j\theta_i(t)], \qquad \text{for } i = 1, 2\,. \tag{30}$$

The effect of the gain is to compensate the phase jitter due to fading, and to weight the signal by a factor that is proportional to the signal strength. Thus, a strong signal carries a larger weight than a weak signal. This optimum combiner is based on the assumption that the channel attenuation $r_i(t)$ and the phase jitter $\theta_i(t)$ are perfectly known. In practice, $r_i(t)$ and $\theta_i(t)$ can be estimated by adaptive equalizers which make use of the continuity of the channel fading [6]. For a fixed set of branches' gains $\{K_i\}$, the output of the maximum ratio combiner at baseband can be expressed equivalently as a single decision variable in the form

$$U(t) = r_1^2(t) + r_2^2(t) + r_1(t)N_1(t) + r_2(t)N_2(t) \tag{31}$$

where $N_i(t)$ is the equivalent low-pass filtered Gaussian white noise in the ith branch. $U(t)$ has a normal distribution with mean $\bar{U}(t)$ equal to

$$\bar{U}(t) = r_1^2(t) + r_2^2(t) \tag{32}$$

and variance $\sigma_U^2(t)$ given by

$$\sigma_U^2(t) = [r_1^2(t) + r_2^2(t)]\,\sigma_N^2 = \bar{U}\sigma_N^2\,. \tag{33}$$

From (3), the PDF of $x_i(t) = r_i^2(t)$ can be derived as

$$p_3(x_i) = \begin{cases} \frac{1}{2b_0\sqrt{2\pi d_0}} \int_0^{\infty} \frac{1}{z} \exp[-\frac{(\ln z-\mu)^2}{2d_0} - \frac{x_i+z^2}{2b_0}] \mathrm{I}_0(\frac{\sqrt{x_i}z}{b_0})\, dz, & x_i \geq 0 \\ 0, & x_i < 0\,. \end{cases} \tag{34}$$

The PDF of the signal component $\bar{U}(t)$ is

$$p_4(\bar{U}) = \int_0^{\bar{U}} p_3(x)\, p_3(\bar{U}-x)\, dx\,. \tag{35}$$

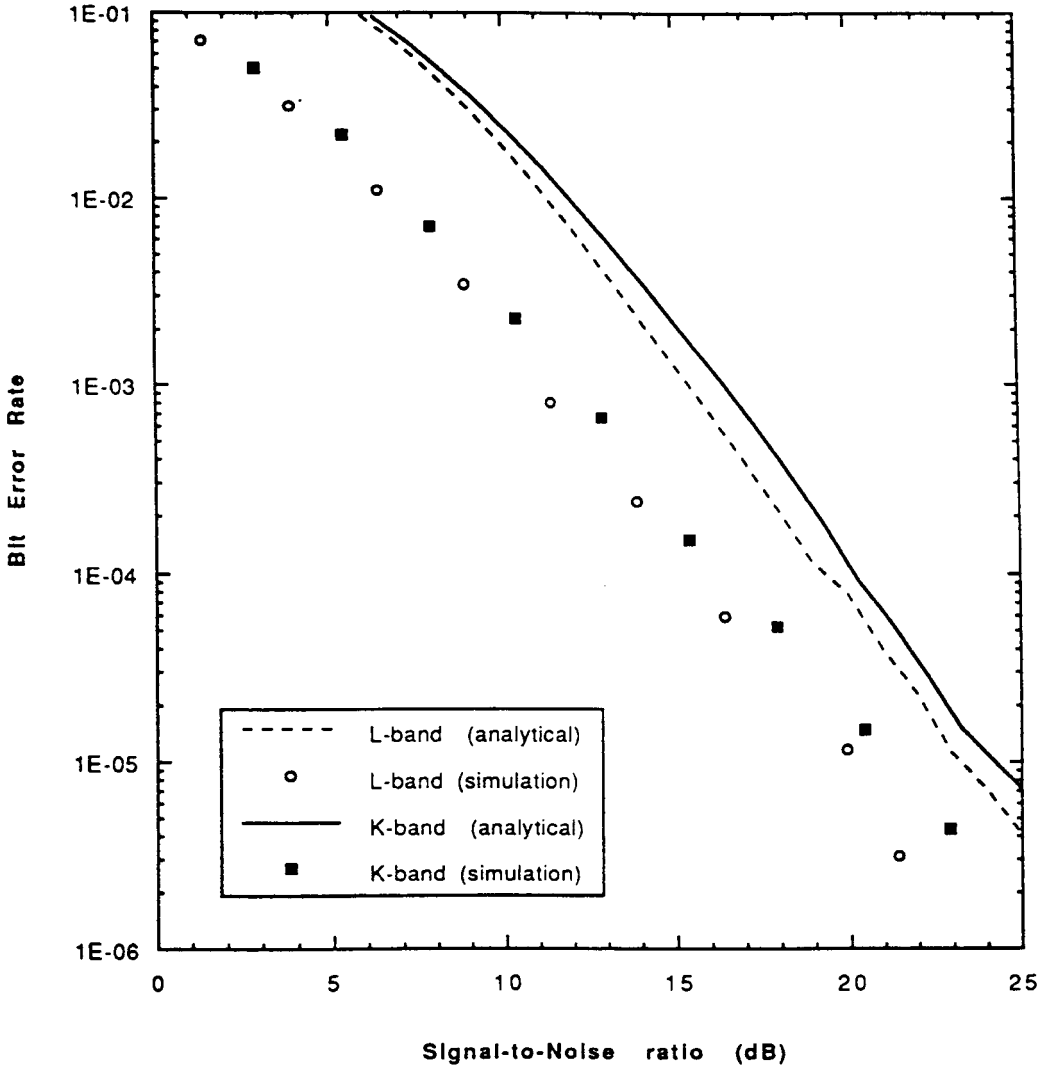

Figure 9. BER of Coherent BPSK in LMS channel with Equal Gain Diversity at L-band and K-band (average shadowing).

Similar to the case of equal gain combining, the upper bound of the average bit error rate is equal to

$$P_e^{av} \leq \frac{1}{2}\int_0^{\infty} \exp\left(-\frac{\bar{U}}{2\sigma_N^2}\right) p_4(\bar{U})d\bar{U} \tag{36}$$

with the input SNR obtained from (29).

Figure 10 shows the BER performance with maximum ratio diversity reception at L and K band. The analytical results are obtained by numerically solving (34) to (36). Compared with that of the equal gain combining (Figure 9), the performance at a BER of 10^{-3}, is improved by approximately 0.5 dB at L band and 2.1 dB at K band respectively.

The performance improvement with diversity reception is summarized in Table 4. It is shown that:

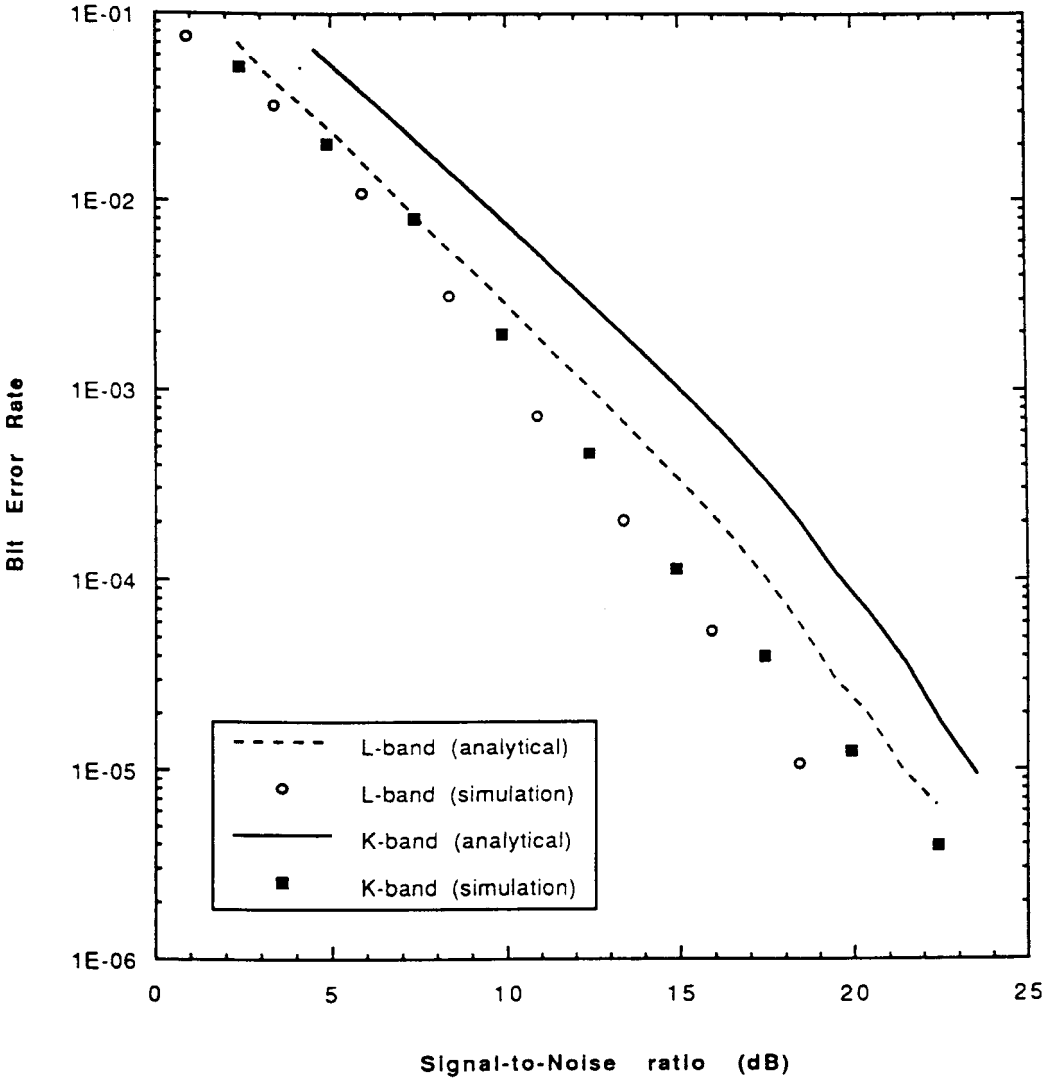

Figure 10. BER of Coherent BPSK in LMS channel with Maximum Ratio Diversity at L-band and K-band (average shadowing).

i) the performance improvement in the case of average shadowing is significant;
ii) the performance at K band is improved more than that at L band;
iii) the performance improvement increases as the BER decreases; and
iv) the maximum ratio combining is better than the equal gain combining.

In addition to diversity reception, channel coding can be used to mitigate channel impairments. Trellis-coded differential M-ary phase-shift-keying with dual-space equal-gain reception has been investigated in [20] based on computer simulation for L-band and K-band land mobile satellite communication system.

In the above analysis, we have applied the frequency scaling technique to study the channel characteristics for the K-band transmission, and have evaluated the BER performance of coherent BPSK over the K-band channel with and without diversity reception.

Table 4. Receiver performance improvement by diversity reception.

P_e	$EG^{\dagger}$-L	EG-K	$MR^{\ddagger}$-L	MR-K
10^{-3}	6.8 dB	8.4 dB	7.3 dB	10.6 dB
10^{-4}	12.1 dB	14.0 dB	12.6 dB	16.1 dB

†Equal gain combining; ‡Maximum ratio combining.

The channel model gives a statistical description of the channel fading at K band. Once extensive measurement data is available to statistically characterize the K-band fading channel, the statistical parameters of the channel model may be further modified accordingly depending on the propagation environments. Based on the analysis and simulation results on different channel fading scenarios (i.e., in the cases of light shadowing, average shadowing, and heavy shadowing) [21], it is expected that, in the case of heavy shadowing, the channel fading statistics and the BER performance (versus averaged received signal-to-noise ratio) are not sensitive to the channel model parameters μ and d_0, because the LOS component is negligible compared with the Rayleigh distributed multipath component. However, the sensitivity of the fading statistics and BER performance to the variation of the channel parameters is expected to increase as the degree of shadowing reduces (such as in the case of light shadowing), where the LOS component plays a dominating role as compared with the multipath component.

5. Conclusions

A comparative study for the land mobile satellite communication system operating at K and L bands has been presented. It has been shown that in the case of average shadowing,

i) the LOS signal component at K band has up to more than 6.0 dB higher attenuation than that at L band;
ii) the channel fades have a much faster rate at K band than at L band;
iii) dual-space diversity mitigates the channel fading by approximately 4.0 to 12.0 dB, depending on fading depth and channel parameters;
iv) diversity reception also improves the second-order statistics of the fading channel by reducing the deep fading durations;
v) channel fading impairments are mitigated more at K band than at L band by the space diversity technique.

An upper-bound for the bit error rate performance of a coherent BPSK system in the LMS channel has been evaluated theoretically and further validated by computer simulations. With multipath fading and shadowing, at a bit error rate of 10^{-3}, at K band, the system loses approximately 3.5 dB more than at L band. At a given BER, the performance improvement of a coherent BPSK system depends on the diversity combining technique employed, the channel propagation conditions and the RF carrier frequency used by the communication system.

Acknowledgements

This work is supported by a strategic grant (STR-0100720) from the Natural Sciences and Engineering Research Council (NSERC) of Canada. The authors would also like to thank Dr. Abbas Yongaçoğlu for his support and many valuable discussions.

References

1. C. Loo, “A Statistical Model for a Land Mobile Satellite Link”, IEEE Trans. on Veh. Tech., vol. 34, pp. 122-127, 1985.
2. J. S. Butterworth, “Propagation Measurements for Land Mobile Satellite System at 1542 MHz,” Communication Research Center, Department of Communications, CRC Technical Note 723, 1984.
3. J. S. Butterworth, “Propagation Measurements for Land Mobile Satellite Services in the 800 GHz Band,” Communication Research Center, Department of Communications, CRC Technical Note 724, 1984.
4. C. Loo, “Digital Transmission Through a Land Mobile Satellite Channel”, IEEE Trans. on Commun., vol. 38, pp. 693-697, 1990.
5. M.A. Weissberger, An Initial Summary of Models for Predicting the Attenuation of Radio Waves by Trees. U.S. Dept. of Defense, Report no. ESD-TR-81-101, 1981.
6. P. Balaban and J. Salz, “Optimum Diversity Combining and Equalization in Digital Data Transmission with Applications to Cellular Radio,” IEEE Trans. Commun., vol. 40, pp. 885-907, 1992.
7. J. Proakis, Digital Communications. Second Edition, New York: McGraw-Hill Book Company, 1989, chap. 4.
8. N.C. Beaulieu, and A. Abu-Dayya, “Analysis of Equal Gain Diversity on Nakagami Fading Channel, ” IEEE Trans. Commun., vol. 39, pp. 225-234, 1991.
9. W.C. Jakes, Microwave Mobile Communication. New York: Wiley, 1974.
10. C. Trabelsi, “RS Codes and Linear Prediction Techniques for Land Mobile Satellite Channels”, M.A.Sc. Thesis, Dept. of Electrical Engineering, University of Ottawa, 1990.
11. A. Papoulis, Probability, Random Variables, and Stochastic Processes. Second Edition, McGraw-Hill International Book Company, 1984.
12. P. Beckmann and A. Spizzichino, The Scattering of Electromagnetic Waves From Rough Surface. Artech House, 1987.
13. R. W. Huck, J. S. Butterworth and E. E. Matt, “Propagation Measurements for Land Mobile Satellite Services”, Proc. 33rd IEEE Veh. Tech. Conf., 1983.
14. K. Dessouky and T. Jedrey, “The ACTS Mobile Terminal”, JPL SATCOM Quarterly, No. 8, pp. 17-23, 1993.
15. C. Loo, “Land Mobile Satellite Channel Measurement at Ka Band Using Olympus”, Proc. 44th IEEE Veh. Tech. Conf., Stockholm, Sweden, 1994.
16. R. M. Barts and W.L. Stutzman, “Modeling and Simulation of Mobile Satellite Propagation,” IEEE Trans. Antennas Propagat., vol. 40, pp. 375-382, 1992.
17. W. J. Vogel and J. Goldhirsh, “Earth-Satellite Tree Attenuation at 20 GHz: Foliage Effects”, IEE Electron. Lett., Vol. 29, No. 18, pp. 1640-1641, 1993.
18. W. Lee, Mobile Communications Engineering. New York: McGraw-Hill, 1982.
19. D. G. Brennan, “Linear Diversity Combining Techniques,” Proc. IRE., vol. 47, pp. 1075-1102, 1959.
20. W. Zhuang, A. Yongacoglu and J.-Y. Chouinard, “Trellis-Coded Differential MPSK with Multiple-Symbol Viterbi Decoder over Shadowed Mobile Satellite Channel at L and K Bands”, Int. J. Sat. Commun., Vol. 13, No. 3, pp.159-169, 1995.
21. W. Zhuang, A. Yongacoglu, J.-Y. Chouinard and D. Makrakis, “Performance analysis of EHF land mobile satellite system – channel modeling and performance of coherent MPSK”, Technical Report, Department of Electrical Engineering, University of Ottawa, 1992.

Weihua Zhuang received the B.Sc. (1982) and M.Sc. (1985) degrees from Dalian Marine University (China) and the Ph.D. degree (1992) from the University of New Brunswick (Canada), all in electrical engineering. From January 1992 to September 1993, she was a Post Doctoral Fellow first at the University of Ottawa and then at Telecommunications Research Labs (TRLabs, Edmonton), working on land mobile satellite communications and indoor wireless communications. Since October 1993, she has been with the Department of Electrical and Computer Engineering, University of Waterloo, where she is an Assistant Professor. Her current research interests include digital transmission over fading channels, wireless networking, and radio positioning.

Dr. Zhuang is a licensed Professional Engineer in the Province of Ontario, Canada.

Jean-Yves Chouinard received B.Sc.A., M.Sc. and Ph.D. degrees in Electrical Engineering from Laval University in 1979, 1984 and 1987 respectively. From 1979 to 1981, he was with Northern Telecom in Montreal, where he was involved in the line-up and testing of the DRS-8 digital microwave radio system. From 1987 to 1988, he was at the Space and Radio communication Division of the Centre National d'Études des Télécommunications (CNET) in France, as a postdoctoral fellow working on the simulation of the GSM mobile radio subsystem. In August 1988, he joined the University of Ottawa, where he is currently an associated professor in the Department of Electrical Engineering. In 1993, he was invited to give a short course on "Secure Communications and Data Encryption" as a guest lecturer at the Jordan University of Science and Technology (JUST), in Irbid, Jordan. His current research interests are mobile radio propagation, in-building propagation, digital channel modelling, as well as error control coding and digital modulation techniques for advanced television systems.

Dimitrios Makrakis received the Diploma from the University of Patras, Patras, Greece in 1982, the M.A. Sc. degree from the University of Toronto, Toronto, Canada in 1984 and the Ph.D. degree from the University of Ottawa, Ottawa, Canada in 1992, all in Electrical Engineering.

From 1985 to 1989 he was with the Department of Electrical Engineering of the University of Ottawa, first as Research Assistant and afterwards (since 1987) as Research Engineer, working in the areas of digital mobile and satellite communications, as well as in multimedia communication networks and BISDN. From 1989 to 1991 he was a Research Scientist with the Communications Research Centre of the Canadian Government, involved in propagation and channel characterization studies in Ka-band for possible use in personal satellite communications. From 1991 to 1993 he was a Research Scientist with Telesat Canada, performing research on networks, communication systems technology and channel characterization aspects for EHF communications. From 1993 to July 1995 he was Research Associate at the Department of Electrical Engineering of the University of Ottawa, where he worked in the areas of design and performance analysis of protocols for BISDN (ATM) networks and personal communication networks as well as on the application of Advanced Intelligent Networks (AIN) technology to the multimedia and personal communications service. He has published more than 15 refereed journal papers and more than 40 conference papers in these areas. He is presently an Assistant Professor with the Department of Electrical Engineering of Lakehead University, Thunder Bay, Canada. His current work is in high speed networks, personal wireless communications and intelligent networks.

Dr. Makrakis received the award of excellent achievements in 1982 from the National Technical Chamber of Greece and in 1985 he held a scholarship from the school of Graduate studies of the University of Ottawa. He is a member of the Technical Chamber of Greece.